A Revised Formulation of Modal Absorbing and Matched Modal Source Boundary Conditions for the Efficient FDTD Analysis of Waveguide Structures

Federico Alimenti, *Associate Member, IEEE*, Paolo Mezzanotte, Luca Roselli, *Member, IEEE*, and Roberto Sorrentino, *Fellow, IEEE*

***Abstract*—A revised formulation of modal absorbing and matched modal source boundary condition is proposed for the efficient analysis of a waveguide circuit with the finite-difference time-domain (FDTD) method. The formulation is based on a suitable translation operator modeling, in time domain, the propagation in a uniform hollow waveguide. By applying this operator, a multimodal absorbing boundary condition is obtained. Moreover, a source algorithm is developed that generates a given incident wave, while absorbing each modal component reflected from a discontinuity. The source is capable to separate incident and reflected waves without requiring any presimulation of long uniform waveguides. The validity and effectiveness of the formulation is verified by means of three numerical experiments. The first two refer to waveguide discontinuities. In these cases, the FDTD results are compared versus mode-matching results. The third example is a transition from waveguide to printed circuit transmission line. The numerical simulation is compared with published experimental results. The presented examples show that the generalized scattering matrix of a waveguide circuit can be evaluated accurately in the smallest computational space allowed by the structure.**

***Index Terms*—FDTD method, generalized scattering matrix, matched modal source, modal absorbing boundary conditions, waveguide circuits, waveguide impulse response, waveguide transitions.**

I. Introduction

In RECENT years, the finite-difference time-domain (FDTD) method [1], [2] has become one of the most popular methods for the analysis of microwave circuits [3]. This method allows the electromagnetic (EM) field to be computed in a discretized space time domain. In microwave engineering applications, however, the knowledge of the EM field distribution is not sufficient by itself, but has to be complemented by that of the scattering parameters of the microwave circuit.

To compute these parameters, three problems must be faced. First, the circuit ports must be properly terminated. Since the most common way to evaluate the scattering parameters is to eliminate the reflected wave by matching the circuit ports, the accuracy of the extraction procedure is strictly dependent on the absorbing boundary conditions (ABC's) used to simulate the matched terminations. In order to minimize the errors due to the imperfect ABC, different approaches have been proposed in [4] and [5].

Second, when the field distribution at the circuit ports results from the superposition of several modal components, in order to compute the scattering parameters it is necessary to identify the dominant mode component. To this purpose, it is useful practice to insert uniform waveguide lengths at the circuit ports in such a way as to eliminate the contribution of higher order modes. This has the price of increasing the computational domain.

Third, incident and reflected waves must be extracted from the total EM field. The conventional approach is based on the separation of incident and reflected pulses in time domain. This method, however, requires a long uniform feeding line, increasing further the computational domain. In order to minimize such a domain, the excitation scheme proposed in [6] can be adopted. Other techniques to obtain the incident wave consist of simulating a uniform waveguide or, alternatively, monitoring the wave propagation at almost three observation points along the waveguide axis [7].

For hollow waveguide structures, the above problems can be solved by expanding the total EM field into waveguide modes and by rewriting the boundary condition at the circuit ports in terms of modal amplitudes. This approach has been exploited to develop a family of boundary conditions suitable for the evaluation of the scattering parameters of a waveguide circuit. Such boundary conditions are referred as to modal absorbing boundary conditions (MABC's) and matched modal source boundary conditions (MMSBC). The MABC [8]–[12] are almost ideal matched terminations [13] and, as shown in [14], can be used very close to a waveguide discontinuity, where the EM field results from the superposition of several modes. The MMSBC has been first proposed in [15] and allows the real-time separation of incident and reflected waves.

In this paper, the formulation of MABC and MMSBC algorithms is revised by introducing a suitable translation operator. The operator is obtained both analytically and numerically, the latter being derived by using a one-dimensional time-domain model of a uniform waveguide [16]. The revised formulation allows the MMSBC proposed in [15] to be extended to a fully multimodal case. Moreover, the incident wave, necessary to the

Manuscript received August 28, 1998.

The authors are with the Institute of Electronics, University of Perugia, I-06125 Perugia, Italy (e-mail: alimenti at istel.ing.unipg.it).

Publisher Item Identifier S 0018-9480(00)00215-5.

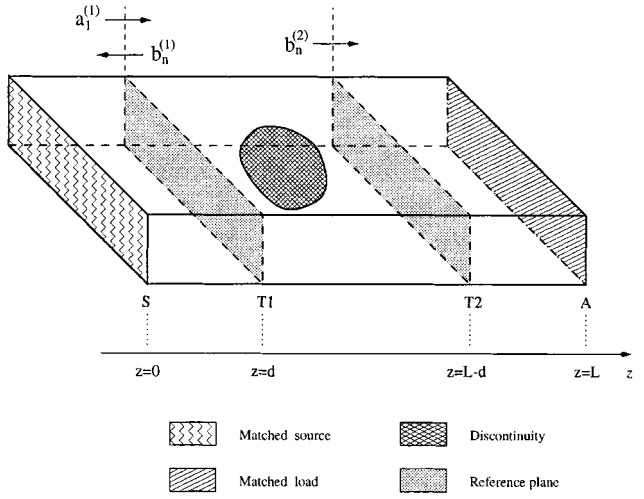

Fig. 1. Two port waveguide discontinuity.

source algorithm, can be computed by means of the translation operator, avoiding the presimulation of a long uniform waveguide. Results are presented in order to validate the MABC and MMSBC algorithms and to show their capabilities in terms of numerical accuracy and computational effort.

Due to the multimodal feature of the algorithms proposed, throughout this paper, rather than simply to the scattering parameters, we will refer, in general, to the computation of the generalized scattering matrix (GSM) of a microwave circuit. The GSM will be introduced in the following section.

II. GSM Computation

Let us consider the generic two-output waveguide discontinuity shown in Fig. 1. The reference planes T_p ($p = 1, 2$) are located across the longitudinal z-axis at coordinates $z_1 = d$ and $z_2 = L - d$.

To calculate the GSM with the FDTD method, the transverse electric field at T_p must be expanded into waveguide modes as follows:

$$\boldsymbol{E}_t^{(p)}(z_p, t) = \sum_{n=1}^{N_p} V_n^{(p)}(z_p, t)\boldsymbol{e}_n^{(p)}. \tag{1}$$

In the above expression, n is the mode index, N_p is the number of modes used in the expansion of the electric field, and $\boldsymbol{e}_n^{(p)}$ is the electric modal vector. The transverse coordinate dependence has been omitted to simplify the notation. The amplitudes $V_n^{(p)}(z_p, t)$ can be viewed as equivalent modal voltages. Note that (1) holds for hollow, or homogeneously filled with no dispersive material, waveguides.

With reference to Fig. 1, incident $a_n^{(p)}$ and reflected $b_n^{(p)}$ voltage waves can be expressed in terms of forward $V_{+,n}^{(p)}$ and backward $V_{-,n}^{(p)}$ voltage waves

$$a_n^{(p)}(z_p, t) = \begin{cases} V_{+,n}^{(p)}(z_p, t), & \text{for } p = 1 \\ V_{-,n}^{(p)}(z_p, t), & \text{for } p = 2 \end{cases} \tag{2}$$

$$b_n^{(p)}(z_p, t) = \begin{cases} V_{-,n}^{(p)}(z_p, t), & \text{for } p = 1 \\ V_{+,n}^{(p)}(z_p, t), & \text{for } p = 2. \end{cases} \tag{3}$$

These relationships allow the total voltage $V_n^{(p)}$ to be expressed as the superposition of incident and reflected voltage waves

$$V_n^{(p)}(z_p, t) = a_n^{(p)}(z_p, t) + b_n^{(p)}(z_p, t). \tag{4}$$

A method to evaluate the GSM consists of terminating the computational FDTD domain by a matched load and matched source. The load (plane A of Fig. 1) must absorb each transmitted wave. The source (plane S of Fig. 1) must excite only one waveguide mode, while absorbing each wave reflected by the discontinuity. If the dominant mode (index $n = 1$) is excited at the first output (index $p = 1$), the following matching/excitation condition must be satisfied:

$$a_n^{(p)}(z_p, t) = \begin{cases} s(t), & \text{for } p = 1 \text{ and } n = 1 \\ 0, & \text{for } p \neq 1 \text{ or } n \neq 1. \end{cases} \tag{5}$$

$s(t)$ being the source strength. The generalization of (5) to the excitation of an arbitrary mode at a generic output is straightforward. In the following section, it will be shown that the boundary condition (5) can be implemented by means of MABC and MMSBC algorithms.

The GSM can be easily computed as follows, by evaluating the Fourier transform of incident and reflected voltage waves:

$$S_{nm}^{(pq)}(\omega) = \frac{\sqrt{\eta_m^{(q)}}}{\sqrt{\eta_n^{(p)}}} \frac{b_n^{(p)}(\omega)}{a_m^{(q)}(\omega)} \tag{6}$$

where

$$\eta_n^{(p)} = \begin{cases} \omega\mu/\beta_n^{(p)} & \text{TE modes} \\ \beta_n^{(p)}/\omega\epsilon & \text{TM modes} \end{cases} \tag{7}$$

with

$$\beta_n^{(p)} = \frac{1}{c_0}\sqrt{\omega^2 - \left(\omega_{c,n}^{(p)}\right)^2} \tag{8}$$

and

$$\omega_{c,n}^{(p)} = c_0\, k_{c,n}^{(p)}. \tag{9}$$

In the previous expressions, $\beta_n^{(p)}$ is the phase constant of the nth mode in the pth waveguide, $\omega_{c,n}^{(p)}$ is the angular cutoff frequency, and c_0 is the velocity of the light. Note that the first factor of (6) normalizes the scattering parameters in such a way as the unitarity and symmetry properties of the GSM are conserved.

III. MABC and MMSBC Algorithms

The MABC and MMSBC algorithms can be easily explained by introducing a suitable translation operator as a model of a uniform hollow waveguide.

Let $V_{+,n}(z, t)$ be the voltage wave traveling forward along the z-axis of a uniform waveguide. The wave amplitude of the nth mode at the location $\overline{z} + d$, with $d \geq 0$, can be expressed in terms of the amplitude at $\overline{z}$ using the translation operator $\mathcal{P}_{n,d}$

$$V_{+,n}(\overline{z} + d, t) = \mathcal{P}_{n,d} V_{+,n}(\overline{z}, t). \tag{10}$$

A symmetric relationship holds for the wave $V_{-,n}(z, t)$, traveling backward along the z-axis

$$V_{-,n}(\overline{z}-d, t) = \mathcal{P}_{n,d} V_{-,n}(\overline{z}, t). \tag{11}$$

These translation relationships can be considered as the formal definition of the linear operator $\mathcal{P}_{n,d}$. Its evaluation will be discussed in the following section.

The translation operator $\mathcal{P}_{n,d}$ applies to each modal amplitude. By using a mode superposition, such an operator allows the modal expansion (1) to be transferred from a plane with longitudinal coordinate $\overline{z}$ to a plane with longitudinal coordinate $\overline{z} \pm d$.

A. MABC Algorithm

The MABC algorithm is illustrated at the example of Fig. 1. In particular, we refer to an MABC at $\overline{z} = 0$ suitable for the absorption of the waves traveling backward along the z-axis. This case will be used to later introduce the matched modal source.

From the knowledge of the total electric field at $\overline{z} = d$ (output index $p = 1$), one obtains the total voltages at the same plane by exploiting the orthogonality of the modal vectors

$$V_n^{(1)}(d, t) = \int_{S_1} \boldsymbol{E}_t^{(1)}(d, t) \cdot \boldsymbol{e}_n^{(1)} \, dS \tag{12}$$

S_1 being the cross section of the first waveguide. Since a matched load has been assumed by hypothesis, $V_{+,n}^{(1)}(d, t) = 0$. Hence,

$$V_{-,n}^{(1)}(d, t) = V_n^{(1)}(d, t). \tag{13}$$

Using (1) and (13) and the translation operator, the electric field at $\overline{z} = 0$ is given by

$$\boldsymbol{E}_t^{(1)}(0, t) = \sum_{n=1}^{N_1} \mathcal{P}_{n,d}^{(1)} V_n^{(1)}(d, t) \boldsymbol{e}_n^{(1)}. \tag{14}$$

This expression constitutes the MABC at $\overline{z} = 0$. The corresponding algorithm is illustrated in Fig. 2. The transverse electric field at $\overline{z} = d$ is expanded in terms of normal modes (12), each modal amplitude is propagated back to $z = 0$ using the translation operator, and then the total electric field at the plane of the MABC ($\overline{z} = 0$) is obtained as the superposition of its modal components (14).

B. MMSBC Algorithm

Consider now the presence of a source at $\overline{z} = 0$ (output index $p = 1$) of Fig. 1. The source is supposed to excite only the fundamental mode of the waveguide and is matched with respect to N_1 modal components reflected by the discontinuity. Let $s(t)$ be the amplitude of the generated incident voltage wave. The transverse electric field at the source plane is the superposition of the source-generated field plus the field (14) reflected by the discontinuity

$$\boldsymbol{E}_t^{(1)}(0, t) = s(t)\boldsymbol{e}_1^{(1)} + \sum_{n=1}^{N_1} \mathcal{P}_{n,d}^{(1)} V_{-,n}^{(1)}(d, t) \boldsymbol{e}_n^{(1)}. \tag{15}$$

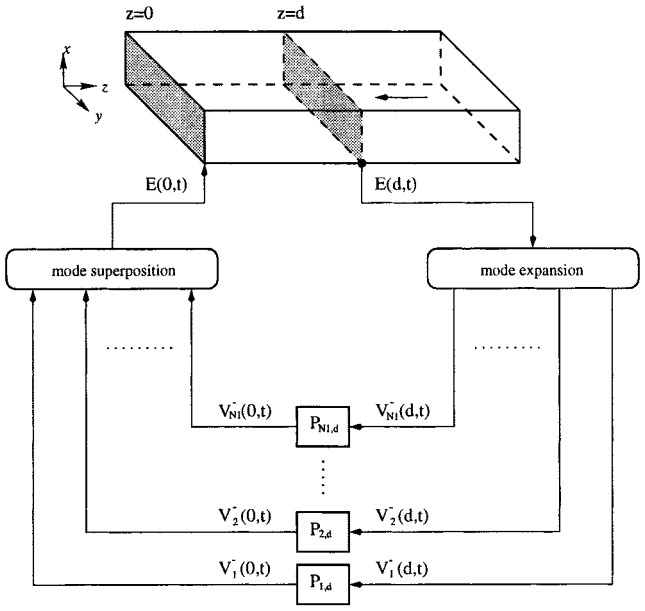

Fig. 2. MABC applied to the waves traveling backward along the z-axis. The boundary condition is imposed at $z = 0$. The field is expanded in modes at $z = d$.

Since the source is supposed to be matched and excites only the dominant mode (index $n = 1$), the backward voltages $V_{-,n}^{(1)}(d, t)$ are related to the total voltages by

$$V_{-,n}^{(1)}(d, t) = \begin{cases} V_1^{(1)}(d, t) - V_{+,1}^{(1)}(d, t), & n = 1 \\ V_n^{(1)}(d, t), & n = 2, \cdots, N_1 \end{cases} \tag{16}$$

where the only unknown is the amplitude $V_{+,1}^{(1)}(d, t)$ of the forward dominant mode. In [15], this quantity has been evaluated by a presimulation (carried out with the three-dimensional FDTD) of a long uniform waveguide. By using the translation operator, the same quantity can be computed as

$$V_{+,1}^{(1)}(d, t) = \mathcal{P}_{1,d}^{(1)} s(t). \tag{17}$$

Combining the above relationships, one finally obtains the expression of the MMSBC at $\overline{z} = 0$

$$\boldsymbol{E}_t^{(1)}(0, t) = \left\{ s(t) + \mathcal{P}_{1,d}^{(1)} \left[V_1^{(1)}(d, t) - \mathcal{P}_{1,d}^{(1)} s(t) \right] \right\} \boldsymbol{e}_1^{(1)} + \sum_{n=2}^{N_1} \mathcal{P}_{n,d}^{(1)} V_n^{(1)}(d, t) \boldsymbol{e}_n^{(1)}. \tag{18}$$

The electric field at $\overline{z} = 0$ is expressed in terms of the modal field amplitudes at $\overline{z} = d$ by means of the modal translation operators $\mathcal{P}_{n,d}^{(1)}$. The matched modal source algorithm is illustrated in Fig. 3. Note that the same structure of Fig. 2 is used to provide the absorption of the reflected waves. Observe that, by using the linearity of the translation operator, (18) can be rewritten as

$$\boldsymbol{E}_t^{(1)}(0, t) = \left[s(t) - \mathcal{P}_{1,2d}^{(1)} s(t) \right] \boldsymbol{e}_1^{(1)} + \sum_{n=1}^{N_1} \mathcal{P}_{n,d}^{(1)} V_n^{(1)}(d, t) \boldsymbol{e}_n^{(1)} \tag{19}$$

where $\mathcal{P}_{1,2d}^{(1)} = \mathcal{P}_{1,d}^{(1)} \mathcal{P}_{1,d}^{(1)}$.

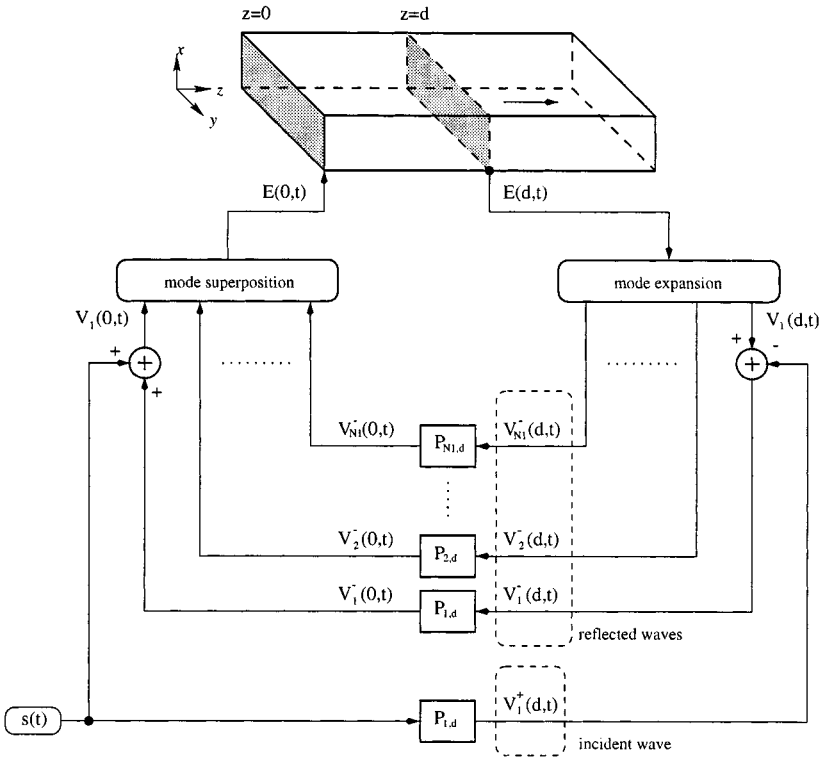

Fig. 3. Matched modal source. In this case, the fundamental mode is excited while the first N_1 modes are absorbed. The source plane is at $z = 0$. Incident and reflected waves are available at the expansion plane $z = d$.

The MABC and MMSBC algorithms can be extended easily to the absorption of waves traveling forward along the z-axis and to arbitrary mode excitation.

IV. Translation Operator

This section is devoted to the computation of the translation operator $\mathcal{P}_{n,\,d}$ which, by definition, transforms the forward (backward) voltage wave $V_{+,\,n}(\overline{z},\,t)$ $(V_{-,\,n}(\overline{z},\,t))$ of the nth waveguide mode into the same quantity evaluated in $\overline{z}+d$ $(\overline{z}-d)$.

In frequency (or Laplace) domain, the translation operator simply correspond to the phase shift introduced by a uniform waveguide of length d as follows:

$$\mathcal{P}_{n,\,d} = H_{n,\,d}(s) \tag{20}$$

where

$$H_{n,\,d}(s) = e^{-\jmath\beta_n d} = e^{-(d/c_0)\sqrt{s^2+\omega_{c,\,n}^2}} \tag{21}$$

is the waveguide transfer function of voltage type [13, p. 247] and $\mathcal{P}_{n,\,d}$ is the translation operator in the Laplace domain. By inverting (20) and (21), one obtains the translation operator in time domain

$$\mathcal{P}_{n,\,d} = h_{n,\,d}(t)* \tag{22}$$

where

$$h_{n,\,d}(t) = \mathcal{L}^{-1}\{H_{n,\,d}(s)\} \tag{23}$$

is the waveguide impulse response and $*$ is the convolution operator. Substituting (22) into (10) and (11) and discretizing time and space with $t = i\Delta t$, $z = j\Delta z$, respectively, the translation relationships becomes

$$V^i_{+,\,n,\,j+1} = h_{n,\,\Delta z}[i] * V^i_{+,\,n,\,j} \tag{24}$$

and

$$V^i_{-,\,n,\,j-1} = h_{n,\,\Delta z}[i] * V^i_{-,\,n,\,j} \tag{25}$$

where a distance $d = \Delta z$ has been assumed. In these expressions, the following notation has been adopted to distinguish between continuous and discrete functions

$$\begin{aligned} h_{n,\,\Delta z}[i] &= h_{n,\,\Delta z}(i\Delta t) \\ V^i_{n,\,j} &= V_n(j\Delta z,\,i\Delta t). \end{aligned} \tag{26}$$

The convolutions (24) and (25) can be evaluated adopting two different approaches, i.e., analytically or numerically. With the first approach, the waveguide impulse response (23) is evaluated first analytically, then discretized in space and time to obtain $h_{n,\,\Delta z}[i]$. As an alternative, the translation relationships can be evaluated through a waveguide numerical simulation performed in a discretized one-dimensional domain.

A. Analytical Impulse Response

The waveguide impulse response can be found by computing (23) analytically. To this purpose, the function (21) must be rewritten as follows:

$$H_{n,\,d}(s) = e^{-\tau s} - \left(e^{-\tau s} - e^{-\tau\sqrt{s^2+\omega_{c,\,n}^2}}\right) \tag{27}$$

where $\tau = d/c_0$ is the propagation time between the excitation and observations points. The inverse Laplace transform of the

first term is a delayed Dirac's impulse, while that of the second can be found in [17, p. 1027]. One obtains

$$h_{n,d}(t) = \delta(t-\tau) - \frac{\omega_{c,n}\tau}{\sqrt{t^2-\tau^2}} \cdot J_1\left(\omega_{c,n}\sqrt{t^2-\tau^2}\right) u(t-\tau) \quad (28)$$

$J_1(x)$ being the Bessel's function of first kind and $u(t)$ the Heaviside (or unitary step) function. The relationship (28) has been derived in [18], in the more general case of waveguide filled with a lossy dielectric.

To construct an MABC or MMSBC algorithm, the impulse response (28) must be discretized in time. The main problem is that the delay τ is not a multiple of the sampling interval Δt. By expressing the delay in terms of integer and fractional parts

$$\tau = (\ell_d + \alpha)\Delta t \quad (29)$$

$$\ell_d = \text{int}\left(\frac{d}{c_0\Delta t}\right) \quad (30)$$

$$\alpha = \frac{d}{c_0\Delta t} - \ell_d \quad (31)$$

the impulse with delay τ can be approximated as the superposition of two impulses with integer delay $\ell_d\Delta t$ and $(\ell_d+1)\Delta t$

$$\delta(t-\tau) \approx (1-\alpha)\delta(t-\ell_d\Delta t) + \alpha\delta(t-(\ell_d+1)\Delta t). \quad (32)$$

Sampling the waveguide impulse response and using (32), one obtains

$$h_{n,d}[i] = (1-\alpha)\delta[i-\ell_d] + \alpha\delta[i-(\ell_d+1)] - \frac{\Delta t\omega_{c,n}\tau}{\sqrt{(i\Delta t)^2-\tau^2}} J_1\left(\omega_{c,n}\sqrt{(i\Delta t)^2-\tau^2}\right) \cdot u(i-(\ell_d+1)). \quad (33)$$

Numerical experiments have demonstrated that the direct application of (33) is not very accurate. For example, an MABC that uses (33) shows a spurious reflection of about −50 dB. This error can be ascribed to the approximation (32) and to the numerical dispersion of the FDTD algorithm altering the phase constant of the waveguide [13, p. 257]. A detailed discussion of this problem is, however, beyond the scope of this paper. To improve the accuracy of MABC and MMSBC algorithms, the impulse response in (23) has been evaluated numerically.

B. Numerical Impulse Response

The numerical impulse response can be determined by representing a hollow uniform waveguide by a set of modal transmission lines as in [16]. The line equation is

$$\frac{\partial^2 V_n}{\partial z^2} - \frac{1}{c_0^2}\frac{\partial^2 V_n}{\partial t^2} - k_{c,n}^2 V_n = 0 \quad (34)$$

n being the mode order and V_n the equivalent modal voltage. This equation is discretized according to a one-dimensional FDTD scheme

$$V_{n,j}^{i+1} = AV_{n,j}^{i} + B\left(V_{n,j+1}^{i} + V_{n,j-1}^{i}\right) - V_{n,j}^{i-1} \quad (35)$$

with

$$A = 2 - \frac{2c_0^2\Delta t^2}{\Delta z^2} - c_0^2\Delta t^2 k_{c,n}^2$$
$$B = \frac{c_0^2\Delta t^2}{\Delta z^2}. \quad (36)$$

Observe that (35) is very fast computing, as it involves only five floating point operations (two multiplications and three summations) per time step. To ensure the stability of (35), the following inequality must be satisfied [19, p. 71]:

$$\Delta t \le \frac{2}{c_0\sqrt{k_{c,n}^2 + \left(\frac{2}{\Delta z}\right)^2}}. \quad (37)$$

The time step Δt given by (37) is greater than that computed according to the Courant's criterion for the three-dimensional FDTD with the same Δz.

To evaluate the impulse response of the nth waveguide mode, the corresponding transmission line must be excited with an impulsive signal at the origin. The time evolution of the equivalent voltage is computed with (34) assuming a semi-infinite line. The impulse response is given by the equivalent voltage at a distance d from the excitation point.

Numerically, a semi-infinite transmission line cannot be simulated. However, as suggested in [8], [13, pp. 251–252], and [20], this problem can be overcome adopting a discrete transmission line with only four nodes. The first node is for the excitation, the second to pick up the impulse response, and the last two for the application of an absorbing algorithm. The latter can use the samples of the impulse response in progress. The numerical computation of the waveguide impulse response is reduced to the following recursive formula:

$i < 2$:

$$h_{n,\Delta z}[0] = 0$$
$$h_{n,\Delta z}[1] = B$$

$i \ge 2$:

$$h_{n,\Delta z}[i] = Ah_{n,\Delta z}[i-1] - h_{n,\Delta z}[i-2] + BV_{n,3}^{i-1}$$
$$V_{n,3}^{i} = AV_{n,3}^{i-1} - V_{n,3}^{i-2} + B\left(V_{n,4}^{i-1} + h_{n,\Delta z}[i-1]\right)$$
$$V_{n,4}^{i} = \sum_{\ell=2}^{i-1} h_{n,\Delta z}[i-\ell]V_{n,3}^{\ell} \quad (38)$$

assuming $V_{n,j}^{i} = 0$ for $i = 0, 1$ and $j = 3, 4$. The accuracy of the MABC and MMSBC algorithms based on the numerical impulse response can be improved by slightly modifying the eigenvalue $k_{c,n}^2$ in (35) according to [13, p. 258].

The number of floating point operations required to the computation of each convolution in (24) or (25) is N_t^2, where N_t is the length of the simulation in number of time steps. For the evanescent modes, this effort can be avoided by evaluating directly the waves at $\overline{z} \pm \Delta z$.

C. Evanescent Modes

For those modes that are evanescent in the whole frequency range considered in the FDTD simulation, a more efficient way

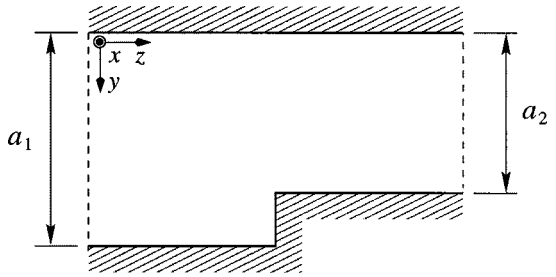

Fig. 4. *H*-plane step. The dimensions and the discretization adopted are: $a_1 = 32\Delta y = 22.86$ mm, $a_2 = 21\Delta y = 15$ mm, $b = 14\Delta x = 10.16$ mm (not shown), $\Delta z = 0.5$ mm, $\Delta t = 1.18$ ps.

can be employed to numerically evaluate the translation relationships (24) and (25). This is accomplished by exciting the nth discrete transmission line with the signal $V^i_{+,n,j}$ (or $V^i_{-,n,j}$) and by shorting it at a distance far enough from the excitation point so that the line voltage has vanished. The translated wave $V^i_{+,n,j+1}$ (or $V^i_{-,n,j-1}$) is the voltage at the second node of the discrete transmission line. The distance between short circuit and excitation point that ensures an amplitude attenuation of A is

$$j_n = \text{int}\left(\frac{c_0 \ln(1/A)}{\Delta z\sqrt{\omega^2_{c,n} - \omega^2_{\max}}}\right) + 1 \tag{39}$$

where $\omega_{\max}$ is the maximum analysis frequency and the distance j_n is expressed in the number of cells. In this paper, $A = 10^{-8}$ has been used. The translated waves can be determined by solving (35) with the following boundary conditions:

$$\begin{cases} V^i_{n,1} = V^i_{+,n,j} \\ V^i_{n,j_n} = 0 \end{cases} \quad \text{or} \quad \begin{cases} V^i_{n,1} = V^i_{-,n,j} \\ V^i_{n,j_n} = 0. \end{cases} \tag{40}$$

Thus, (24) and (25) become

$$V^i_{+,n,j+1} = V^i_{n,2} \quad \text{or} \quad V^i_{+,n,j-1} = V^i_{n,2}. \tag{41}$$

The number of floating point operations involved in this procedure is $5N_t(j_n - 2)$, which increases linearly with the length of the simulation [13, p. 259].

V. Results

To check the validity and effectiveness of the proposed formulation, three numerical experiments are presented here. The first two examples refer to waveguide discontinuities. In these cases, the generalized scattering parameters computed by the FDTD simulations are compared versus mode-matching results. The third example is a waveguide-to-microstrip transition. The FDTD simulation is compared with the experimental results presented in [21].

A. H-Plane Step

The *H*-plane step of Fig. 4 has been considered as a first example [22]. A uniform mesh has been adopted for the spatial discretization. The dimension of the structure and discretization parameters are indicated in the caption. An MMSBC absorbing the first seven modes has been applied at the wider waveguide and the smaller one has been terminated with an MABC matched with respect to the first five modes.

In order to validate the method in the most critical case, the computational volume has been reduced to only four cells along the z-axis. The excitation $s(t)$ is a 11.5-GHz cosinusoidal signal modulated with a Gaussian pulse having a 7-GHz bandwidth. Observe that, beyond 13 GHz, two modes can propagate in the wider waveguide.

The GSM has been computed according to the procedure described in Section II. The elements $S^{(11)}_{nm}$ with $n, m = 1, 2, 3$, i.e., the generalized scattering parameters between pairs of modes at the output $p = 1$, are shown in Fig. 5 and compared with the mode-matching simulations. The agreement is excellent.

The size of the computational volume is: 14 × 32 × 4 cells. Three simulations are necessary to evaluate the submatrix $[S_{11}]$ of size 3 × 3. Each simulation takes about 120 s for 8000 time steps. The computation has been performed on a Pentium II 233-MHz platform, with 64 MB of RAM, and Linux operating system.

The use of MABC and MMSBC allows us to analyze the discontinuity beyond the frequency of 13 GHz, i.e., beyond the onset of higher order mode propagation in the wider waveguide.

B. E-Plane Mitered Bend and Corner

The *E*-plane mitered bend of Fig. 6 has been considered as a second example. A uniform mesh has been adopted for the spatial discretization along with the triangular cell approximation described in [23]. The dimension of the structure and discretization parameters are indicated in the caption.

An MMSBC absorbing the first five $\text{TE}_{1n}/\text{TM}_{1n}$ modes has been applied at the input waveguide and the output has been terminated with an MABC using the same modal set. The excitation $s(t)$ is a 12.5-GHz cosinusoidal signal modulated with a Gaussian pulse having a 5-GHz bandwidth.

The magnitude of S_{11} for two values of d/b are shown in Fig. 7. In the figure, the frequency axis has been normalized with respect to the cutoff frequency $f_c = 7.87$ GHz of the waveguide. Fig. 7(a) refers to a mitered bend with $d/b = 0.87$. This result has been compared with the mode-matching analysis discussed in [24] and with the boundary contour mode-matching method (BCMM) introduced in [25]. Fig. 7(b) refers to a corner with $d/b = \sqrt{2}$. Also in these cases, a very good agreement is observed.

The size of the computational volume is: 16 × 16 × 27 cells. The computation time is of about 28 s for 2000 time steps.

C. Waveguide-to-Microstrip Transitions

The proposed algorithm can also be applied to compute the scattering parameters of transition from waveguide to printed circuit transmission lines. In such cases, a perfectly matched layer (PML) can be used to terminate the computational domain at the printer circuit side.

As an example, consider the waveguide-to-microstrip transition shown in Fig. 8. The dimensions of the structure are quoted in the caption of the figure. A study of this discontinuity has been reported in [21].

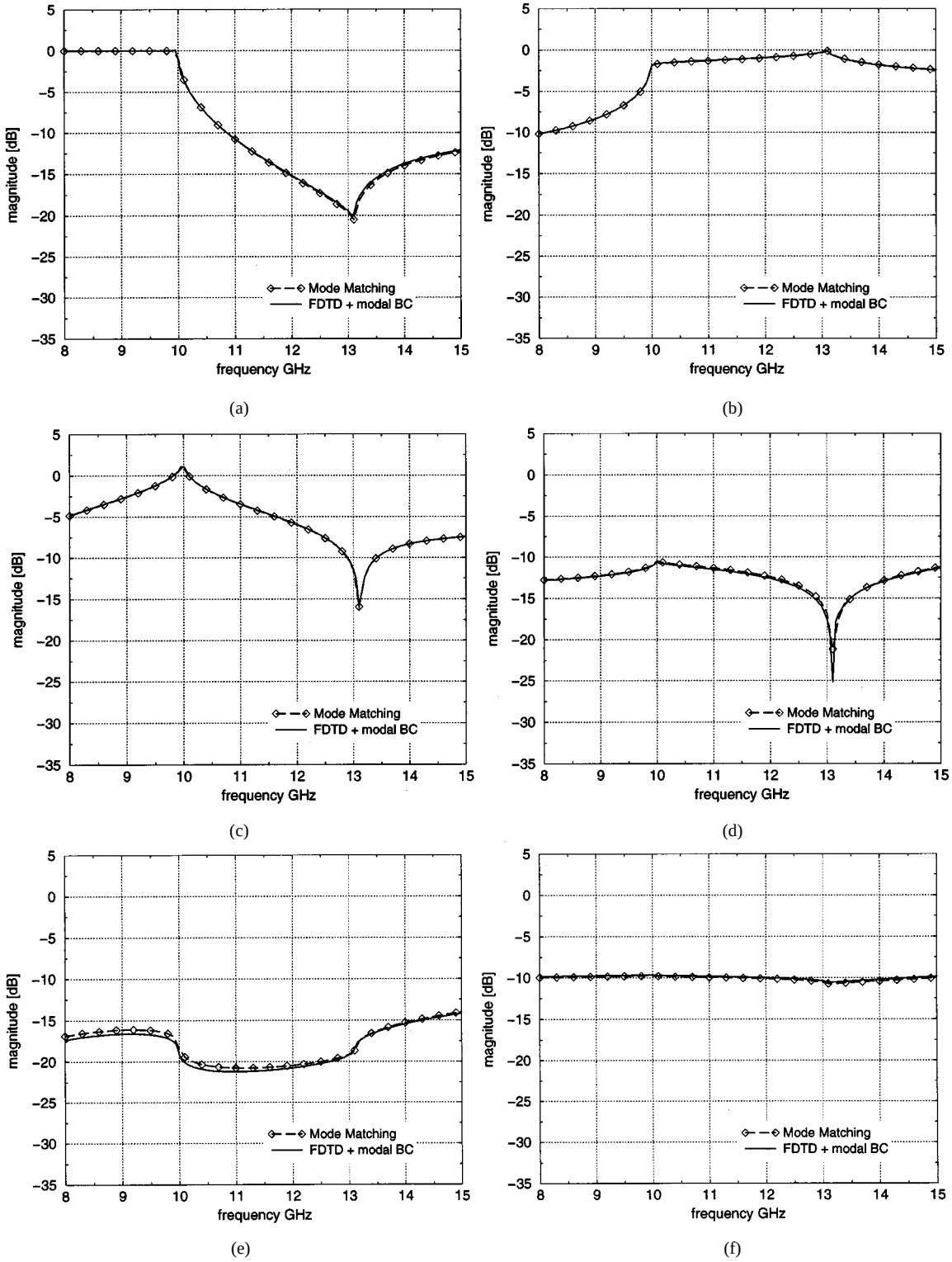

Fig. 5. GSM of the *H*-plane step. Comparison between FDTD and mode matching. The first 3 × 3 elements of the $[S_{11}]$ submatrix are represented in the figure. (a) $S_{11}^{(11)}$ (reflected TE_{10}, incident TE_{10}). (b) $S_{22}^{(11)}$ (reflected TE_{20}, incident TE_{20}). (c) $S_{21}^{(11)}$ (reflected TE_{20}, incident TE_{10}). (d) $S_{32}^{(11)}$ (reflected TE_{30}, incident TE_{20}). (e) $S_{31}^{(11)}$ (reflected TE_{30}, incident TE_{10}). (f) $S_{33}^{(11)}$ (reflected TE_{30}, incident TE_{30}).

A graded mesh [26] with $\Delta x_{\min} = 0.159$ mm, $\Delta y_{\min} = 0.250$ mm, and $\Delta z_{\min} = 0.250$ mm has been adopted for the discretization of the structure. The cell sizes have been varied according to [27], using an increment factor $q \leq 1.4$ in all grid directions. The time step was $\Delta t = 0.39$ ps.

An MMSBC has been applied to the waveguide port. The source absorbs the first seven TE/TM modes reflected by the transition. The microstrip port has been terminated with a PML ABC [28] with a thickness of ten cells, $\sigma_{\max} = 5.0$ S/m and order $n = 4$.

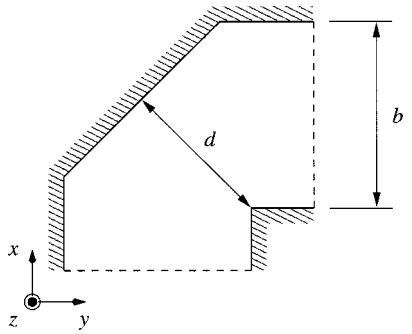

Fig. 6. *E*-plane mitered bend. The dimensions and discretization adopted are: $a = 26\Delta z = 19.05$ mm (not shown), $b = 13\Delta y = 9.525$ mm, $\Delta x = \Delta y$, $\Delta t = 1.4$ ps.

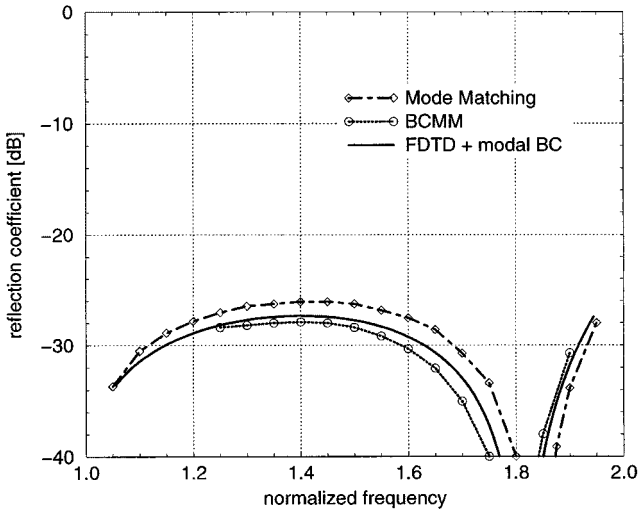

(a)

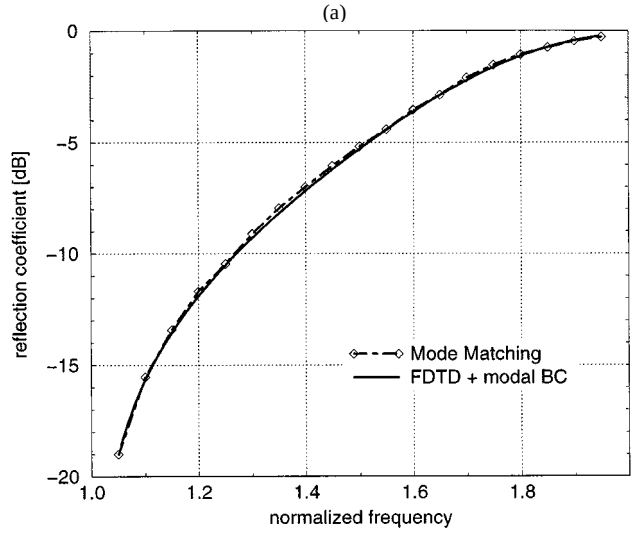

(b)

Fig. 7. S_{11} of (a) the *E*-plane mitered bend with $d/b = 0.87$ and (b) of the *E*-plane corner. Comparison among FDTD, mode-matching, and BCMM methods. The frequency has been normalized with respect to the cutoff frequency of the waveguide.

The reflection coefficient of the waveguide-to-microstrip transition is shown in Fig. 9. This result is in good agreement with the experimental data provided by Machac *et al.*in [21]. The size of the computational space is 29 × 85 × 69 cells and the simulation takes about 56 min for 7000 time steps.

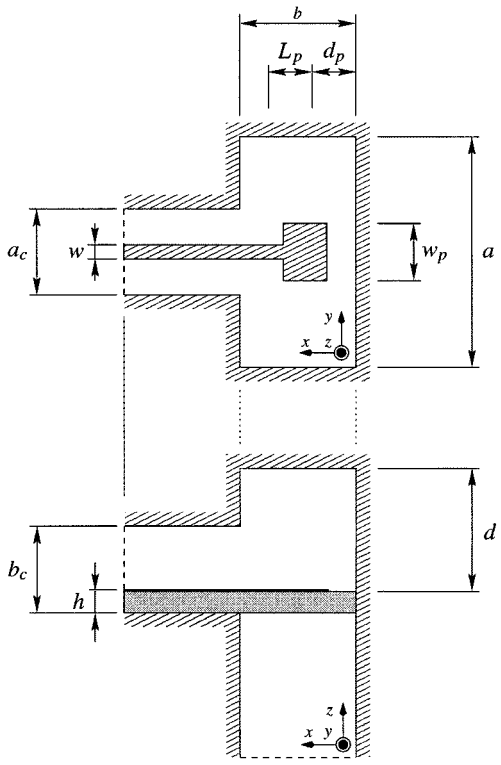

Fig. 8. Waveguide to microstrip transition. The dimensions of the structure are: $a = 22.86$ mm, $b = 10.16$ mm, $d = 5.30$ mm, $a_c = 8.00$ mm, $b_c = 5.00$ mm, $w = 2.30$ mm, $h = 0.79$ mm, $w_p = 9.00$ mm, $L_p = 5.00$ mm, $d_p = 1.00$ mm, $\epsilon_r = 2.35$.

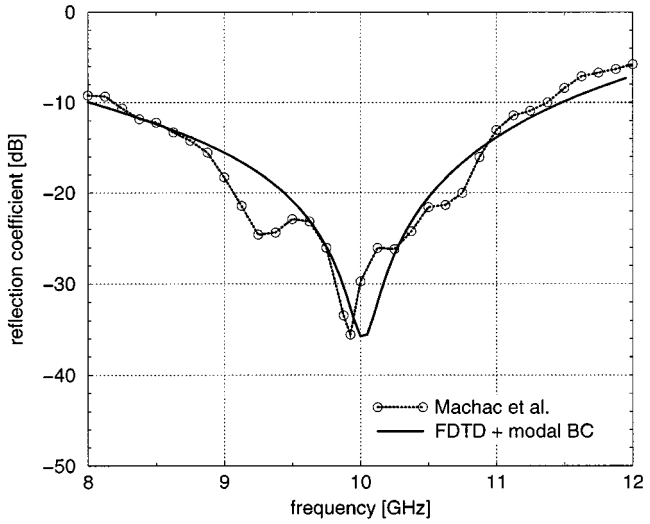

Fig. 9. Magnitude of the reflection coefficient of the waveguide-to-microstrip transition. Comparison between experiment (by Machac *et al.*) and FDTD.

VI. Conclusions

The GSM of a waveguide circuit with arbitrary shape can be computed accurately by incorporating the MABC and MMSBC algorithms into an FDTD simulator. This approach is numerically very efficient since it reduces the FDTD computational domain to the smallest volume allowed by the structure. A revised formulation has been used to derive the MABC and MMSBC. The formulation is based on a suitable translation operator that

models, in time domain, the propagation in a uniform hollow waveguide.

ACKNOWLEDGMENT

The authors wish to acknowledge Prof. F. Alessandri for providing all the mode matching data, and Dr. M. Cryan and Dr. J. Pereda for the interesting discussions and helpful suggestions.

REFERENCES

[1] K. S. Yee, "Numerical solution of initial boundary value problems involving Maxwell's equation in isotropic media," *IEEE Trans. Antennas Propagat.*, vol. 14, pp. 302–307, May 1966.

[2] A. Taflove and M. E. Brodwin, "Numerical solution of steady-state electromagnetic scattering problems using the time-dependent Maxwell's equations," *IEEE Trans. Microwave Theory Tech.*, vol. MTT-23, pp. 623–630, Aug. 1975.

[3] A. Taflove, *Computational Electrodynamics*. Norwood, MA: Artech House, 1995.

[4] J. Ritter, V. J. Branković, D. V. Krupežević, and F. Arndt, "A wide-band s-parameter extraction procedure for arbitrarily shaped, inhomogeneous structures using time domain numerical techniques," in *IEEE Int. Microwave Symp. Dig.*, vol. 1, Orlando, FL, May 1995, pp. 273–276.

[5] F. Moglie, S. Amara, T. Rozzi, and E. Martelli, "De-embedding correction for imperfect absorbing boundary conditions in FD-TD," *IEEE Microwave Guided Wave Lett.*, vol. 6, pp. 37–39, Jan. 1996.

[6] A. P. Zhao and A. V. Raisanen, "Application of a simple and efficient source excitation technique to the FDTD analysis of waveguide and microstrip circuits," *IEEE Trans. Microwave Theory Tech.*, vol. 44, pp. 1535–1539, Sept. 1996.

[7] M. A. Schamberger, S. Kosanovich, and R. Mittra, "Parameter extraction and correction for transmission lines and discontinuities using the finite-difference time-domain method," *IEEE Trans. Microwave Theory Tech.*, vol. 44, pp. 919–925, June 1996.

[8] C. Eswarappa, P. M. So, and W. J. R. Hoefer, "New procedures for 2-D and 3-D microwave circuit analysis with the TLM method," in *IEEE Int. Microwave Symp. Dig.*, Dallas, TX, 1990, pp. 611–664.

[9] F. Moglie, T. Rozzi, P. Marcozzi, and A. Schiavoni, "A new termination condition for the application of FDTD techniques to discontinuity problems in close homogenous waveguide," *IEEE Microwave Guided Wave Lett.*, vol. 2, pp. 475–477, Dec. 1992.

[10] M. Mrozowski, M. Niedźwiecki, and P. Suchomski, "A fast recursive highly dispersive absorbing boundary condition using time domain diakoptics and Laguerre polynomials," *IEEE Microwave Guided Wave Lett.*, vol. 5, pp. 183–185, June 1995.

[11] E. Tentzeris, M. Krumpholtz, N. Dib, and L. B. Katehi, "A waveguide absorber based on analytic Green's functions," in *25th European Microwave Conf.*, Bologna, Italy, Sept. 1995, pp. 251–254.

[12] M. Werthen, M. Rittweger, and I. Wolff, "Multi-mode simulation of homogeneous waveguide components using a combination of the FDTD and FD2 method," in *25th European Microwave Conf.*, Bologna, Italy, Sept. 1995, pp. 234–237.

[13] F. Alimenti, P. Mezzanotte, L. Roselli, and R. Sorrentino, "Modal absorption in the FDTD method: A critical review," *Int. J. Numer. Modeling*, vol. 10, pp. 245–264, 1997.

[14] L. A. Vielva, J. A. Pereda, A. Pietro, and A. Vegas, "FDTD multimode characterization of waveguide devices using absorbing boundary conditions for propagating and evanescent modes," *IEEE Microwave Guided Wave Lett.*, vol. 4, pp. 160–162, June 1994.

[15] T. W. Hunang, B. Houshmand, and T. Itoh, "Efficient modes extraction and numerically exact matched sources for a homogeneous waveguide cross-section in a FDTD simulation," in *IEEE Int. Microwave Symp. Dig.*, vol. 1, San Diego, CA, May 1994, pp. 31–34.

[16] F. Alimenti, P. Mezzanotte, L. Roselli, and R. Sorrentino, "Efficient analysis of waveguide components by FDTD combined with time domain modal expansion," *IEEE Microwave Guided Wave Lett.*, vol. 5, pp. 351–353, Oct. 1995.

[17] M. Abramowitz and I. Stegun, *Handbook of Mathematical Functions*. New York, NY: Dover Publications, 1970.

[18] S. Dvorak, "Exact, closed-form expression for the transient fields in homogeneously filled waveguides," *IEEE Trans. Microwave Theory Tech.*, vol. 42, pp. 2164–2170, Nov. 1994.

[19] M. Mrozowski, "Eigenfunction expansion techniques in the numerical analysis of inhomogeneously loaded waveguide and resonators," *Elektronika*, no. 81, pp. 3–154, 1994.

[20] M. Werthen, M. Rittweger, and I. Wolff, "FDTD simulation of waveguide junctions using a new boundary condition for rectangular waveguides," in *24th European Microwave Conf.*, vol. 24, Cannes, France, Sept. 1994, pp. 1715–1719.

[21] J. Machac and W. Menzel, "On the design of waveguide-to-microstrip and waveguide-to-coplanar line transitions," in *23rd European Microwave Conf.*, Madrid, Spain, Sept. 1993, pp. 615–616.

[22] A. Weisshaar, M. Mongiardo, and V. K. Tripathi, "CAD-oriented equivalent circuit modeling of step discontinuities in rectangular waveguides," *IEEE Microwave Guided Wave Lett.*, vol. 6, pp. 171–173, Apr. 1996.

[23] P. Mezzanotte, L. Roselli, and R. Sorrentino, "A simple way to model curved surfaces in FDTD algorithm avoiding staircase approximation," *IEEE Microwave Guided Wave Lett.*, vol. 5, pp. 267–269, Aug. 1995.

[24] F. Alessandri, M. Mongiardo, and R. Sorrentino, "Rigorous mode matching analysis of mitered *E*-plane bends in rectangular waveguide," *IEEE Microwave Guided Wave Lett.*, vol. 4, pp. 408–410, Dec. 1994.

[25] J. M. Reiter and F. Arndt, "A full-wave boundary contour mode-matching method (BCMM) for the rigorous CAD of single and cascaded optimized *H*-plane and *E*-plane bends," in *IEEE Int. Microwave Symp. Dig.*, San Diego, CA, May 1994, pp. 1021–1024.

[26] D. H. Choi and V. Hoefer, "A graded mesh FD-TD algorithm for eigenvalue problems," in *17th European Microwave Conf.*, Rome, Italy, Sept. 1987, pp. 413–417.

[27] W. Heinrich, K. Beilenhoff, P. Mezzanotte, and L. Roselli, "Optimum mesh grading for finite-difference method," *IEEE Trans. Microwave Theory Tech.*, vol. 44, pp. 1569–1574, Sept. 1996.

[28] S. D. Gedney, "An anisotropic perfectly matched layer-absorbing medium for the truncation of FDTD lattices," *IEEE Trans. Microwave Theory Tech.*, vol. 44, pp. 1630–1639, Dec. 1996.

Federico Alimenti (S'91–A'93) was born in Foligno, Italy, on May 4, 1968. He received the electronic engineering degree (*cum laude*) in electronic engineering and the Ph.D. degree in electronic engineering from the University of Perugia, Perugia, Italy, in 1993 and 1997, respectively.

In 1993, he was with the Microwave and Millimeter-Wave Department, Daimler Benz Aerospace (DASA), Ulm, Germany. In 1997, he visited the Technical University of München, Munich, Germany, under the Vigoni Programme. Since 1993, he has been with the Institute of Electronics, University of Perugia. He was Guest Scientist at the Lehrstuhl für Hochfrequenztechnik of the Technical University of München, Germany. His research interests concern the FDTD simulation of microwave and millimeter-wave devices, the study of monolithic-microwave integrated-circuit (MMIC) interconnection and packaging technologies and the design, realization, and measurement of high-frequency circuits.

Dr. Alimenti was the recipient of a DASA scholarship. He was the recipient of a 1996 Young Scientist Award presented by the Union Radio-Scientifique Internationale.

Paolo Mezzanotte was born in Perugia, Italy, in 1965. He received the Laurea degree in electronic engineering from the University of Ancona, Ancona, Italy, in 1991. His thesis was on FDTD analysis of the GTEM cell. He received the Ph.D. degree from the University of Perugia, Perugia, Italy, in 1997.

Since 1992, he has been involved with FDTD analysis of microwave structures in cooperation with the Institute of Electronics, University of Perugia. His main field of interest is the application of numerical methods to the study of components and structures for microwave and millimeter-wave circuits.

Luca Roselli (M'93) was born in Firenze, Italy, in 1962. He received the Laurea degree in electronic engineering from the University of Firenze, Firenze, Italy, in 1988.

From 1988 to 1991, he was with the University of Firenze, where he was involved with SAW devices. In November 1991, he joined the Institute of Electronics, University of Perugia, Perugia, Italy, as a Research Assistant, and since 1994, he holds the course of Electronic Devices. His research interests include the design and development of millimeter-wave and microwave active and passive circuits by numerical techniques.

Roberto Sorrentino (M'77–SM'84–F'90) received the Doctor degree in electronic engineering from the University of Rome "La Sapienza," Rome, Italy, in 1971.

In 1971, he joined the Department of Electronics, University of Rome "La Sapienza," where he became an Assistant Professor in 1974. He was also a Professore Incaricato at the University of Catania (1975–1976), University of Ancona (1976–1977), and University of Rome "La Sapienza" (1977–1982), where he was then an Associate Professor (1982–1986). In 1983 and 1986, he was appointed as a Research Fellow at the University of Texas at Austin. From 1986 to 1990, he was a Professor at the Second University of Rome "Tor Vergata." Since November 1990, he has been a Professor at the University of Perugia, Perugia, Italy, where he was the Chairman of the Electronic Institute and Director of the Computing Center and is currently the Dean of the Faculty of Engineering. His research activities have been concerned with EM wave propagation in anisotropic media, interaction with biological tissues, and mainly with the analysis and design of microwave and millimeter-wave passive circuits. He has contributed to the planar-circuit approach for the analysis of microstrip circuits and to the development of numerical techniques for the modeling of components in planar and quasi-planar configurations. He is on the Editorial Board of the *International Journal of Numerical Modeling* and the *International Journal of Microwave and Millimeter-Wave Computer-Aided Engineering*.

Dr. Sorrentino is a member of the Editorial Boards of the IEEE TRANSACTIONS ONMICROWAVE THEORY AND TECHNIQUES.